S1. Materials

Fe_3O_4 nanoparticles (specific surface area: 81.98 m^2/g, > 99.5 %), as MNPs, was purchased from US Research Nanomaterials and stirred in deionized water for a day and then was separated by centrifugation, filtered, dried, and finally stored in a vacuum oven (50 °C, 40 mm Hg). Acrylic acid (AA, Merck, 99 %) and 2-hydroxyethyl methacrylate (HEMA, Merck, 99 %) was passed through a basic alumina column to remove the polymerization inhibitor before use. N-isopropylacrylamide (NIPAAM, Sigma-Aldrich, 97 %), fluorescein isothiocyanate (FITC, Sigma-Aldrich, ≥ 90 %), (3-aminopropyl)triethoxysilane (APTES, Sigma-Aldrich, ≥ 98 %), tetraethyl orthosilicate (TEOS, Sigma-Aldrich, 98 %), N,N′-methylenebis(acrylamide) (MBA, Sigma-Aldrich, 99 %), azobisisobutyronitrile (AIBN, Acros, 99 %), 2-bromoisobutyryl bromide (BIBB, Sigma-Aldrich, 98 %), Cu(I)Br (Sigma-Aldrich, 98 %), N,N,N′,N″,N″-Pentamethyldiethylenetriamine (PMDETA, Sigma-Aldrich, 99%), bis(thiobenzoyl)disulfide (Sigma-Aldrich, 99 %), copper powder (Cu(0), Sigma-Aldrich, 99.5 %), Folic acid (FA, Sigma-Aldrich, 97 %), N-hydroxysuccinimide (NHS, Merck, 99 %), cysteamine hydrochloride (Sigma-Aldrich, 99 %), maleic anhydride (Merck, 99 %), glycine (Sigma-Aldrich, 99 %), N,N'-carbonyldiimidazole (CDI), N,N'-dicyclohexylcarbodiimide (DCC, Merck, 99 %), triethylamine (TEA, Sigma-Aldrich, 99.5 %), ammonia solution (25 %, Mojallali), ethanol (Sigma-Aldrich, ≥ 99.8 %), *n*-hexane (Sigma-Aldrich, 95 %), acetonitrile (Sigma-Aldrich, 99.8 %), toluene (Merck, 99 %), dimethyl sulfoxide (DMSO, Sigma-Aldrich, ≥ 99.5 %), diethyl ether (Sigma-Aldrich, ≥ 99 %), acetic acid (Sigma-Aldrich, ≥ 99 %), hydrochloric acid (HCl, Mojallali, 37%), ethyl acetate (Sigma-Aldrich, 99.8 %), tetrahydrofuran (THF, Merck, 99 %), dimethylformamide (DMF, Sigma-Aldrich, 99.8 %) and basic alumina (Fluka) was used as received.

S2. Preparation of FITC-APTES

The FITC-APTES was prepared following a previously described method [S1]. APTES was amino-modified by fluorescein isothiocyanate as depicted in Scheme S1. To this end, a solution of APTES/ethanol (5 mL/25 mL) was added to a solution of FITC/ethanol (0.050 g/15 mL) and the reaction was performed for 24 h at room temperature and dark room conditions. The FITC-APTES adduct was stored at 4 ºC and dark room conditions until used.

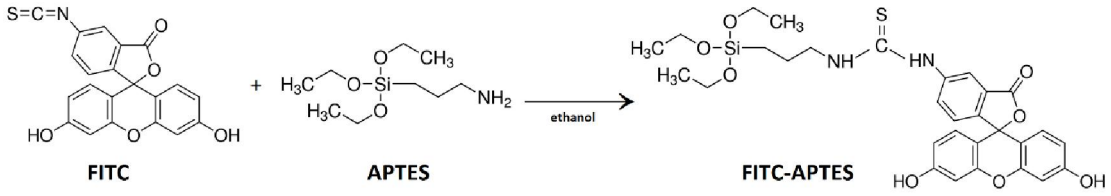

Scheme S1: Synthesis route of FITC-APTES

To realize the synthesis of FITC-APTES, FT-IR analysis was used. According to FT-IR spectrum of APTES (Figure S1-a), characteristic peaks at wavenumbers of 765, 1100, 1280 and 1620 cm^{-1} are related to N-H wag, Si-O-C bonds, stretching C-N and bending N-H vibrations respectively. The FTIR spectrum of FITC (Figure S1-b) shows the characteristic –N=C=S peak at 2100-2150 cm^{-1}. Also, characteristic peak of aromatic -OH groups and ether bonds are located at 3160 and 1105 cm^{-1} respectively. Furthermore, aromatic keto groups of FITC show a peak around 1715 cm^{-1} merged with the peak of acidic carbonyl groups at 1700 cm^{-1}. Complete disappearance of –N=C=S peak in FITC-APTES spectrum (Figure S1-c) can be the main reason to realize the reaction between FITC and APTES and synthesize of FITC-APTES.

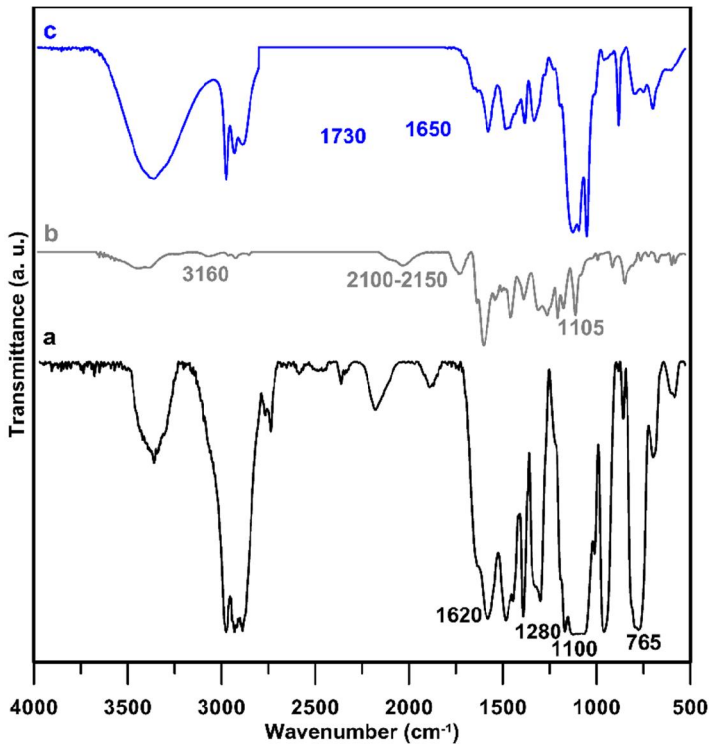

Figure S1: FT-IR spectra of a) APTES, b) FITC and c) FITC-APTES

S3. Synthesis of RAFT agent

Although atom transfer radical polymerization (ATRP) is the most investigated controlled radical polymerization technique [S2-S3], it is uncontrolled in polymerization of acid-functional monomers such as acrylic acid [S4-S5]. Synthesis of (tert)-butyl acrylate [S6] and the subsequent selective deprotection reaction by trifluoroacetic acid or trimethylsilyl iodide leads to PAA. However, the incomplete deprotection and the cleavage of other ester bonds [S7] are the main problems. To solve this problem, reversible addition-fragmentation chain-transfer (RAFT) polymerization [S8-S9] seems to be more applicable. However, the synthesis of RAFT end-functionalized initiators is not so facile. The possibility to convert ATRP initiators, which are readily accessible, into RAFT mediators using a simple methodology would be of great value [S10-S11].

To synthesize RAFT agent from ATRP initiator, 2-bromoisobutyryl bromide (8.4 mL, 0.6 mmol), Cu(0) (1.180 g, 0.018 mol) and bis(thiobenzoyl)disulfide (0.200 g, 0.6 mmol) were dispersed in 50 mL toluene. Then, a mixture of CuBr (0.372 g, 2.6 mmol) and PMDETA (1.2 mL, 1.000 g) were added to the reactor and temperature was raised to 40 °C and reaction was continued for 24 h at nitrogen atmosphere. The resulting dark brown mixture was passed through alumina column to remove Cu compounds and obtain a purple mixture. The final product was dried for 24 h at 40 °C in vacuum oven. The reaction mechanism is depicted in Scheme 4. Copper contents of synthesized RAFT agent was determined as 0.8 ppm via atomic absorption spectrometer (AAS).

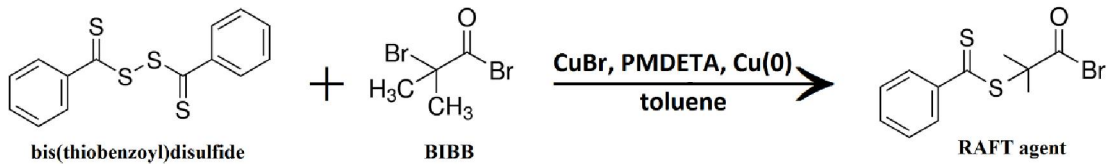

Scheme S2. The synthesis reaction of RAFT agent from ATRP initiator

^{1}H NMR (DMSO-d_6): 2.1 ppm (-C(C**H**$_3$)$_2$-, 6H), 7.1-7.3 ppm (aromatic ring, 5H)

S4. Synthesis of FA-NHS

To synthesis FA-NHS, a previously described method was used [S12]. FA (1.100 g, 2.2 mmol) and TEA (0.5 mL) were dispersed in 50 mL DMSO and after adding a mixture of NHS (4.5 mmol) and DCC (2.4 mmol), reaction was performed for 24 h at dark room conditions. To remove side product (dicyclohexylurea), reaction mixture was filtered

via glass wool to obtain a light yellow mixture. Then, an orange-colored gel was obtained after adding a large amount of diethyl ether. Finally, after filtration, the final product was dried for 48 h at 40 °C in vacuum oven and kept at -20 ºC. The reaction mechanism is depicted in Scheme S3.

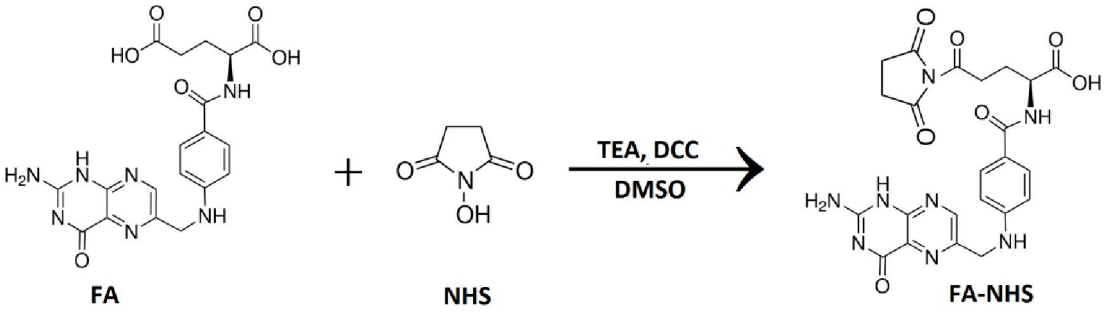

Scheme S3: Synthesis route of FA-NHS

S5. Synthesis of folate-cysteamine (folate-SH)

To synthesis folate-SH, a previously described method was used [S13]. Cysteamine hydrochloride (0.059 g, 0.8 mmol) and TEA (0.2 mL) were added to a mixture of FA-NHS in DMSO (20 mL) and reaction was performed for 24 h at room temperature. Yellow-colored product was reprecipitated via large amount of diethyl ether. The final product was washed by means of deionized water several times and dried for 48 h at 40 °C in vacuum oven. The reaction mechanism is depicted in Scheme S4.

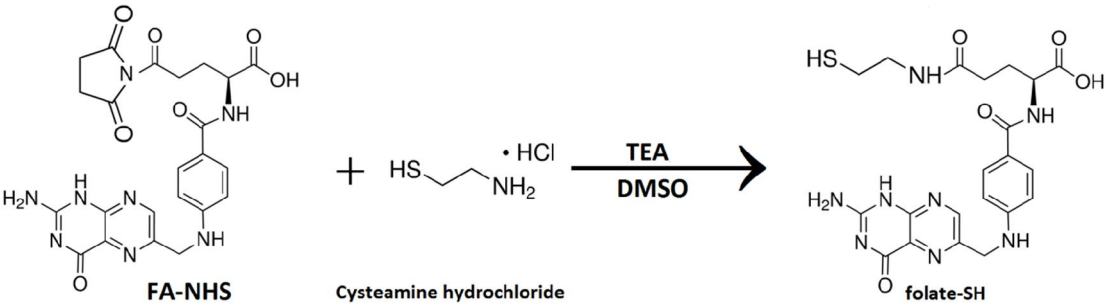

Scheme S4: Synthesis route of folate-SH

S6. Synthesis of N-glycinylmaleimide (GMI)

To synthesis GMI, a previously described method was used [S14]. A solution of maleic anhydride (10.450 g, 0.1065 mol) and glycine (8.000 g, 0.1065 mol) in acetic acid (100 mL) was stirred for 3 h to produce glycidyl maleic acid (GMA). GMA was filtered and washed with deionized water and purified via recrystallization. Then, GMA (2.910 g) was dispersed in toluene (100 mL) and TEA (4.900 g) was added. The mixture was stirred and refluxed for 2 h while the produced water was removed from system. Then, product-containing toluene was separated from produced brown-colored oil. Toluene was evaporated and after adding HCl, pH was reached to 2 and extraction was performed via ethyl acetate. The final product dried for 48 h at 40 °C in vacuum oven. The reaction mechanism is depicted in Scheme S5.

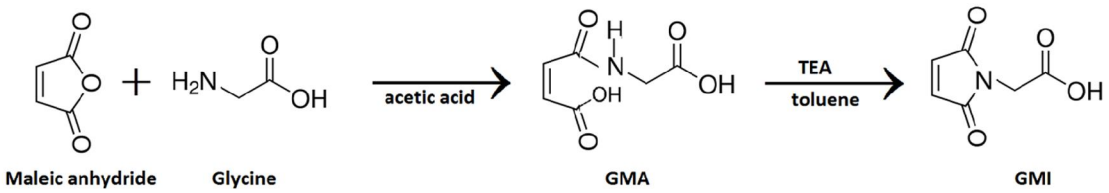

Scheme S5: Synthesis route of GMI

S7. Drug release kinetics

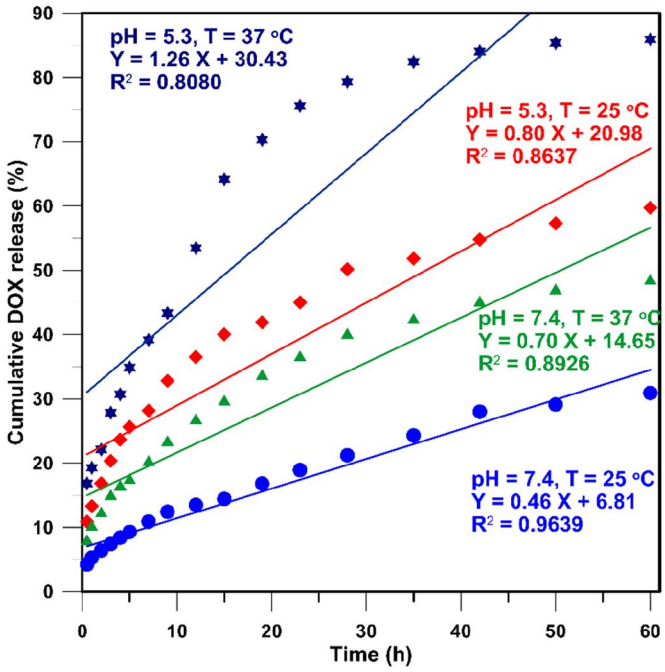

Figure S2: The curve of zero-order model mechanism of drug release

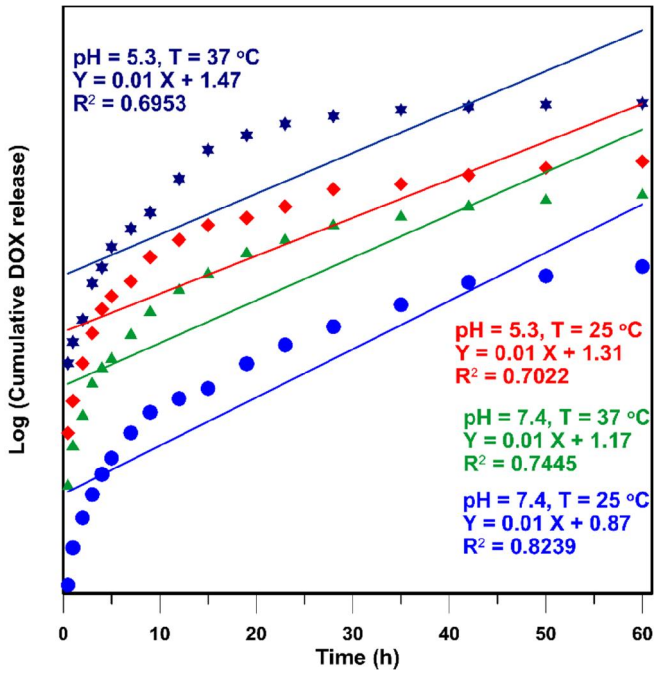

Figure S3: The curve of first-order model mechanism of drug release

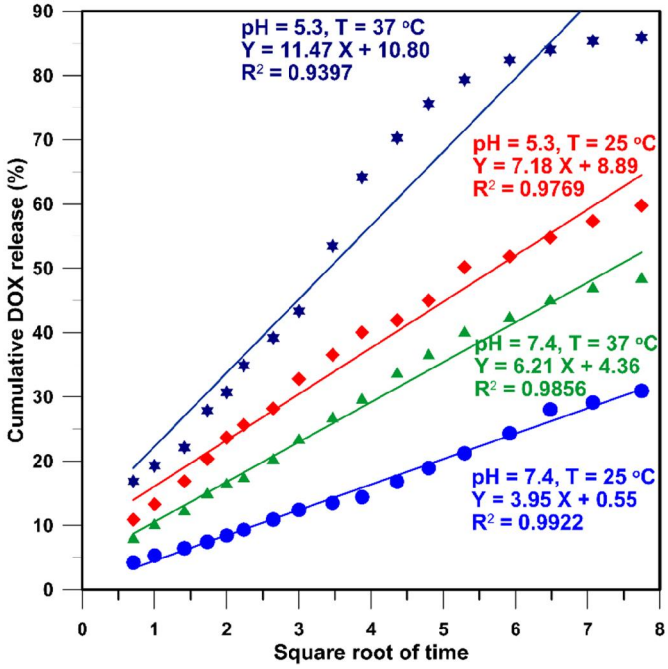

Figure S4: The curve of Higuchi model mechanism of drug release

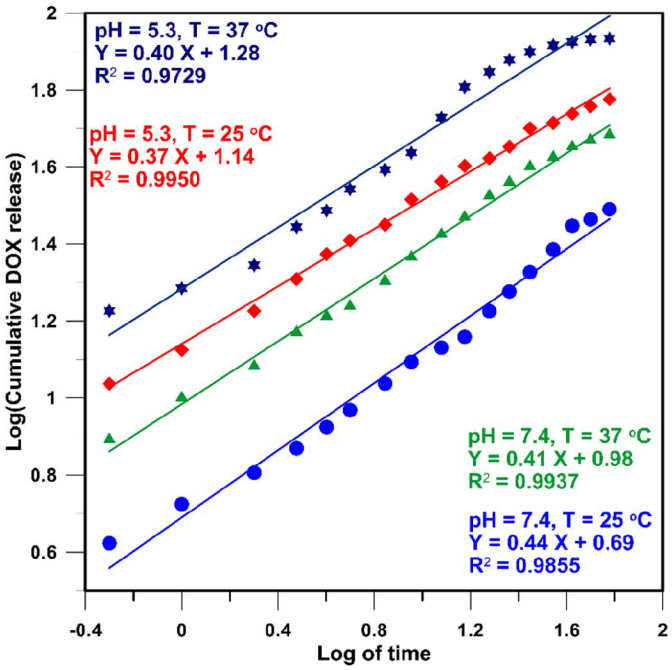

Figure S5: The curve of Korsmeyer-Peppas model mechanism of drug release

S8. Instrumentation

Transmission electron microscope (TEM), Tescan Mira, with an accelerating voltage of 120 kV was used to study the morphology of the nanoparticles. All the samples were prepared by a drop-dry method on carbon-coated copper grids. Fourier transform infrared (FT-IR) spectra were recorded on a Bruker Tensor 27 FT-IR-spectrophotometer, within a range of 500-4000 cm^{-1} using a resolution of 4 cm^{-1}. An average of 24 scans has been carried out for each sample. The samples were prepared on a KBr pellet in vacuum desiccators under a pressure of 0.01 torr. Thermal gravimetric analyses were carried out with a PL thermo-gravimetric analyzer (Polymer Laboratories, TGA 1000, UK). The thermograms were obtained from ambient temperature to 600 °C at a heating rate of 10 °C/min. A sample weight of about 10 mg was used for all the measurements, and nitrogen was used as the purging gas at a flow rate of 50 mL/min. The magnetic properties were obtained using a vibrating sample magnetometer (VSM 7400 Lake Shore, U.S.A.). A dried sample weight of about 10 mg was used for all the measurements. X-ray diffraction (XRD) spectra were collected on an X-ray diffraction instrument (Siemens D5000) with a Cu target ($\lambda = 0.1540$ nm) at room temperature. The system consists of a rotating anode generator which operated at 35 kV and 20 mA. The samples were scanned from $2\theta = 10$ to 80 ° at the step scan mode. The diffraction pattern was recorded using a scintillation counter detector. Ultraviolet-visible (UV-vis.) spectra from liquid samples were recorded on a Perkin-Elmer Lambda 9 instrument. The

concentration of nanoparticles was 0.1 mg/mL. The thermoresponsive and pH-sensitive behaviors of the different samples were investigated by UV-visible absorptions at 600 nm. The concentration of nanoparticles was 0.1 mg/mL of water. The measurement was done after the samples were dispersed in deionized water and allowed to be thermally stable for 1 h. ^{1}H NMR (300 MHz) spectra were recorded on a Bruker Avance 300 spectrometer using deuterated dimethyl sulfoxide (DMSO-d_6) as solvent and tetramethylsilane (TMS) as an internal standard. The copper content of synthesized RAFT agent was determined via an atomic absorption spectrometer (Varian Australia, AA 280). A calibration of 5 different concentrations of a standard provided by a special supplier was done. Then, after drying sample, it dissolved in HNO_3 for AAS analysis.

References

[S1] Antonín Hlavacek, Andreas Sedlmeier, Petr Skladal, and Hans H. Gorris, Electrophoretic Characterization and Purification of Silica-Coated Photon-Upconverting Nanoparticles and Their Bioconjugates, ACS Appl Mater Interfaces 2014, 6, 6930-6935.

[S2] Roghani-Mamaqani, H.; Haddadi-Asl, V.; Khezri, K.; Zeinali, E.; Salami-Kalajahi, M. In Situ Atom Transfer Radical Polymerization of Styrene to in-plane Functionalize Graphene Nanolayers: Grafting through Hydroxyl Groups. J. Polym. Res. 2014, 21, 333.

[S3] Hatami, L.; Haddadi-Asl, V.; Ahmadian-Alam, L.; Roghani-Mamaqani, H.; Salami-Kalajahi, M. Effect of Nanoclay on Styrene and Butyl Acrylate AGET ATRP in Miniemulsion: Study of Nucleation Type, Kinetics, and Polymerization Control. Int. J. Chem. Kinet. 2013, 45, 221-235.

[S4] Ladaviére, C.; Dörr, N.; Claverie, J. P. Controlled Radical Polymerization of Acrylic Acid in Protic Media. Macromolecules. 2001, 34, 5370-5372.

[S5] Patten, T. E.; Matyjaszewski, K. Atom Transfer Radical Polymerization and the Synthesis of Polymeric Materials. Adv. Mater. 1998, 10, 901.

[S6] Ma, Q.; Wooley, K. L. The Preparation of t-Butyl Acrylate, Methyl Acrylate, and Styrene Block Copolymers by Atom Transfer Radical Polymerization: Precursors to Amphiphilic and Hydrophilic Block Copolymers and Conversion to Complex Nanostructured Materials. J Polym. Sci. Pol. Chem. 2000, 38, 4805-4820.

[S7] Javakhishvili, I.; Hvilsted, S. Gold Nanoparticles Protected with Thiol-Derivatized Amphiphilic Poly(ε-caprolactone)-b-poly(acrylic acid). Biomacromolecules. 2009, 10, 74.

[S8] Sobani, M.; Haddadi-Asl, V.; Mirshafiei-Langari, S.-A.; Salami-Kalajahi, M.; Roghani-Mamaqani, H.; Khezri, K. A Kinetics Study on the In Situ Reversible Addition–Fragmentation Chain Transfer and Free Radical Polymerization of Styrene in Presence of Silica Aerogel Nanoporous Particles. Des. Monomers Polym. 2014, 17, 245-254.

[S9] Mehdi Salami-Kalajahi, Vahid Haddadi-Asl, Farid Behboodi-Sadabad, Saeid Rahimi-Razin, and Hossein Roghani-Mamaqani, Effect of silica nanoparticle loading and surface modification on the kinetics of RAFT polymerization, J Polym Eng, 2012, 32, 13-22.

[S10] Rowe, M. D.; Hammer, B. A. G.; Boyes, S.; G. Synthesis of Surface-Initiated Stimuli-Responsive Diblock Copolymer Brushes Utilizing a Combination of ATRP and RAFT Polymerization Techniques. Macromolecules. 2008, 41, 4147.

[S11] Pourya Panahian, Mehdi Salami-Kalajahi, Mahdi Salami Hosseini, Synthesis of Dual Thermosensitive and pH-Sensitive Hollow Nanospheres Based on Poly(acrylic acid-b-2-hydroxyethyl methacrylate) via an Atom Transfer Reversible Addition–Fragmentation Radical Process, Ind. Eng. Chem. Res. 2014, 53, 8079-8086.

[S12] Se-Lim Kim, Hwan-Jeong Jeong, Eun-Mi Kim, Chang-Moon Lee, Tae-Hyoung Kwon, and Myung-Hee Sohn, Folate Receptor Targeted Imaging Using Poly (ethylene glycol)-folate: In Vitro and In Vivo Studies, J Korean Med Sci, 2007, 22 (3), 405-411.

[S13] Francesca Mastrotto, Paolo Caliceti, Vincenzo Amendola, Sara Bersani, Johannes Pall Magnusson, Moreno Meneghetti, Giuseppe Mantovani, Cameron Alexander, and Stefano Salmaso, Polymer control of ligand display on gold nanoparticles for multimodal switchable cell targeting, Chem. Commun., 2011, 47, 9846-9848.

[S14] Zeng Yu-Xiang, Bei Feng-Li, Wang Chao, Yang Xu-Jie, Lu Lu-De, Wang Xin, Synthesis and Quantum Chemical Calculation of N-(4-Sulfophenyl)maleimide and Its Polymer, Acta Chim. Sinica, 2006, 64 (10), 1079-1084.